Numerical solution of the coupled-cluster single- and double-excitation equations with application to Be and Li^-

Sten Salomonson and Per Öster
Department of Physics, Chalmers University of Technology and University of Göteborg, S-412 96 Göteborg, Sweden
(Received 27 December 1989)

An implementation of the coupled-cluster single- and double-excitation (CCSD) method is presented. The CCSD equations are expressed in form of a system of coupled one-particle and two-particle equations. The complete expressions of these equations in terms of Goldstone diagrams are given. Also presented is a simplified diagrammatic notation corresponding to an efficient evaluation scheme. By using numerical discrete spectra to solve these equations, a high numerical accuracy, better than 1 μhartree, is obtained. The method is tested on Be and Li^- and is found to account for 99.3% and 99.4% of the correlation energy, respectively. The CCSD method is demonstrated to give total energies depending very little on the potential used to define the perturbation expansion.

I. INTRODUCTION

In two recent papers a method to obtain finite discrete spectra of the one-particle Schrödinger[1] and Dirac[2] equations has been presented. These spectra were tested to calculate the total energy of the ground state of helium and an accuracy of a few parts in 10^8 was achieved. In this paper we present an implementation of the coupled-cluster single- and double-excitation (CCSD) method using the discrete spectra to solve the system of coupled equations obtained in this method. The CCSD method is applied on Be and Li^-.

The coupled-cluster method was introduced into quantum chemistry by Čížek.[3] Since then several approximation schemes have been developed to take into account the most important clusters. The earlier approximations neglected the single-excitation cluster and were therefore restricted to use of Hartree-Fock orbitals to get reasonable results. The first implementation of the CCSD method, with complete inclusion of the singles and doubles, was presented in 1982 by Purvis and Bartlett.[4] They were later followed by others[5–7] and now also implementations including the triple-excitation cluster, the CCSDT method,[8,9] exist. The implementations referenced above are all mainly intended for molecular calculations and are based on the use of analytical basis sets of Gaussian or Slater-type orbitals. One problem with using such basis sets is that often the error due to the incompleteness of the basis set is hard to estimate and is sometimes larger than neglected physical effects. The method used in the present work does not suffer from such problems since there is a systematic way to increase the numerical accuracy by simply increasing the number of radial lattice points used. Also with analytical basis sets there are now methods available to extend the basis set in a systematic way.[10]

The first application in atomic physics of Goldstone's formulation of many-body perturbation theory was done by Kelly[11] on Be. The Be system has since then very often been used to test new theoretical methods (e.g., Refs. 12–16). The reason for this is that it is the simplest nontrivial many-body system and that very good estimates of the total energy exist. One problem with Be is the well-known degeneracy of $2s^2\,{}^1S$ and $2p^2\,{}^1S$ leading to a large mixing between these configurations (see, e.g., Ref. 12). The best estimate to date of the total energy of Be was done by Bunge[13] from a configuration-interaction (CI) calculation with carefully made estimations of truncation effects.

The CCSD method and its implementation are presented in diagrammatic form in Sec. II. Nonrelativistic applications on Be and Li^- are extensively discussed in Sec. III. The CCSD result should be rather insensitive to the choice of potential used to define the one-particle spectra since all effects of single excitations are included. The difference in the result using different potentials occurs mainly through the effect of the triple excitations which depends slightly on the potential used. This is investigated in the case of Be comparing results using the ordinary Hartree-Fock potential and a Hartree-Fock-Slater potential. A short summary and some conclusions are given in Sec. IV.

II. THE COUPLED-CLUSTER METHOD

The present work is based on the coupled-cluster (CC) method which naturally occurs from many-body perturbation (MBPT) theory by working with the connected parts of the wave-operator diagrams. The CC method originates from nuclear physics (for a review see Ref. 17) and was introduced into quantum chemistry by Čížek.[3] For a detailed description valid for a general open-shell system see the textbook by Lindgren and Morrison.[18] Here a brief description is given, needed to discuss how the implementation of the method has been done. This has been done for a general open-shell system although the results given in Sec. III are for closed-shell systems. For an open-shell application of the present implementation see the calculation of transition probabilities and hyperfine structure of Li.[19]

A wave operator Ω can be defined that transforms model states Ψ_0^a from the model space to states Ψ^a that are exact solutions to the Schrödinger equation

$$\Psi^a=\Omega\Psi_0^a,\quad H\Psi^a=E^a\Psi^a,\quad a=1,\ldots,d\ . \tag{1}$$

The model space is defined by d eigenfunctions to some approximate Hamiltonian H_0, usually chosen to be a central-field Hamiltonian consisting of one-electron operators. The model states are the projections of the exact states onto the model space

$$\Psi_0^a=P\Psi^a \tag{2}$$

where P is the model space-projection operator. The corresponding projection operator for the remaining orthogonal space is denoted by Q and thus

$$P+Q=1\ . \tag{3}$$

The exact energies and the corresponding model states can be found from the wave operator by diagonalizing an effective Hamiltonian H_{eff}

$$H_{\text{eff}}\Psi_0^a=E^a\Psi_0^a \tag{4}$$

where, using intermediate normalization $\langle\Psi_0^a|\Psi^a\rangle=\langle\Psi_0^a|\Psi_0^a\rangle=1$,

$$H_{\text{eff}}=PH\Omega P=PH_0P+W,\quad W=PV\Omega P \tag{5}$$

and using the model states so obtained the exact states can be achieved from Ω.

The difference V between the exact Hamiltonian and H_0 is using MBPT treated as a perturbation and can be separated into zero-, one-, and two- particle parts[18]

$$V=V_0+V_1+V_2\ , \tag{6a}$$

$$V_1=\sum_{i,j}\{a_i^\dagger a_j\}\langle i|v|j\rangle\ , \tag{6b}$$

$$V_2=\tfrac{1}{2}\sum_{i,j,k,l}\{a_i^\dagger a_j^\dagger a_l a_k\}\langle ij|r_{12}^{-1}|kl\rangle\ . \tag{6c}$$

In Figs. 1(a) and 1(b) the graphical representations of V_1 and V_2 are given.

In the CC method the wave operator Ω is written in exponential form

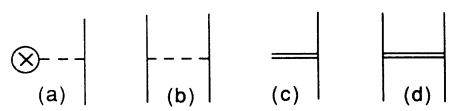

FIG. 1. Diagrammatic notation for the one-body V_1 (a) and two-body V_2 (b) parts of the perturbation and one-body S_1 (c) and two-body S_2 (d) parts of the cluster operator. The vertical lines denote electron lines and the horizontal lines the interactions. The circle with a cross denotes the direct and exchange interaction with the core electrons minus the interaction with the one-particle potential defining the perturbation expansion. The dashed line in (b) denotes the Coulomb interaction. The horizontal double lines in (c) and (d) for the cluster operator indicate that several perturbation interactions are included to give the self-consistent solution of the cluster equation.

$$\Omega=\{\exp(S)\}=P+S+\tfrac{1}{2}\{S^2\}+\cdots \tag{7}$$

where S is the cluster operator and the curly brackets denote antisymmetrization. The cluster operator can be shown to satisfy the following cluster equation:[20]

$$[S,H_0]=Q(V\Omega-\Omega W)_c \tag{8}$$

where the subscript c denotes that only connected diagrams are retained. Also W, defined in Eq. (5), is connected since all clusters describe excitations into the Q space and thus has to be closed by V. As for the perturbation V the cluster operator can be separated into n-particle clusters

$$S=S_1+S_2+S_3+\cdots\ , \tag{9a}$$

$$S_1=\sum_{a,r}\{a_r^\dagger a_a\}s_a^r\ , \tag{9b}$$

$$S_2=\tfrac{1}{2}\sum_{a,b,r,s}\{a_r^\dagger a_s^\dagger a_b a_a\}s_{ab}^{rs}\ . \tag{9c}$$

In this work only the one-particle (single excitations) and the two-particle (double excitations) clusters have been considered but all contributing powers of them are included. This corresponds to the CCSD approximation. The part of Ω contributing to the cluster equation [Eq. (8)] is then

$$\Omega=P+S_1+S_2+\frac{1}{2!}\{S_1^2\}+\{S_1S_2\}+\frac{1}{3!}\{S_1^3\}+\frac{1}{2!}\{S_2^2\}+\frac{1}{2!}\{S_1^2S_2\}+\frac{1}{4!}\{S_1^4\}\ . \tag{10}$$

The cluster operators S_1 and S_2 are represented graphically as in Figs. 1(c) and 1(d).

From Eq. (8) the cluster equation for S_1 is achieved:

$$[S_1,H_0]=Q\left[V_1+VS_1+VS_2+\frac{1}{2!}V\{S_1^2\}+V_2\{S_1S_2\}+\frac{1}{3!}V_2\{S_1^3\}-S_1W_1\right]_{1,c} \tag{11}$$

where the subscript 1 denotes that only single excitations are retained. W_1 can be evaluated as the P projection of the right-hand side (RHS) of Eq. (11) before it is projected onto Q,

$$W_1=P\left[V_1+VS_1+VS_2+\frac{1}{2!}V\{S_1^2\}+V_2\{S_1S_2\}+\frac{1}{3!}V_2\{S_1^3\}\right]_{1,c}\ . \tag{12}$$

Only one-, two-, and three-body excitations in Ω contribute to the S_1 equation, i.e., the last three terms in Eq. (10) do not contribute.

All diagrams contributing to the RHS of Eq. (11) are given in Fig. 2. No arrows have been drawn on the incoming and outgoing electron lines. Depending on what kind of excitation the S_1 cluster describes, the incoming

electron line can be either a valence line usually denoted by a double arrow or a core line usually denoted by a single arrow line directed downwards. Similarly the outgoing line can represent either a virtual electron or, for core excitations, a valence line. There are quite a number of diagrams due to all the terms with different powers of S_1 in Eq. (11). Their evaluation, however, can be systemized considerably by defining new incoming and outgoing orbitals with the S_1 excitations added and a new potential interaction, as shown in Fig. 3. This leads to the simplified diagrammatic S_1 equation given in Fig. 4. The diagram in Fig. 4(a) accounts for 12 diagrams from Fig. 2 labeled (a1)–(a12) and it takes about the same effort to evaluate as the diagram in Fig. 2(a1). The labels of the diagrams in Figs. 2 and 4 give easily the correspondence between the simplified and the full diagrammatic equations.

The practical procedure to evaluate the RHS of Eq. (11) is to first evaluate the nonprojected RHS from the old cluster operators with the definition of incoming orbital lines and potential interaction from Figs. 3(b) and 3(c). Then the overlaps of the RHS with the core orbitals are calculated and these overlaps times the corresponding S_1 excitations are subtracted, which takes the definition of the outgoing lines in Fig. 3(a) into account. Finally the overlaps towards valence orbitals of the RHS's corresponding to valence excitations are calculated, and these overlaps times the corresponding S_1 valence excitations are subtracted which takes the backward diagram in Fig. 4(h) into account.

The cluster equation for S_2 is in the CCSD approximation

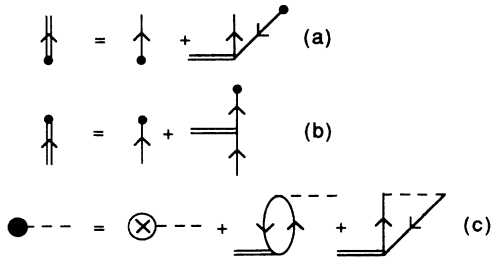

FIG. 3. Simplifying notation used in Figs. 4 and 6. Outgoing double lines denote that the single-particle excitations from core orbitals are added as shown in (a). Incoming double lines denote that the single-particle excitation from the corresponding orbital is added as shown in (b). The incoming lines can be either core lines which should be directed downwards or valence lines usually denoted with double arrows directed upwards but here both cases are indicated with single arrow lines directed upwards. Finally in (c) a new potential interaction is defined including also the linear part of the direct and exchange interaction with the single excitations from below.

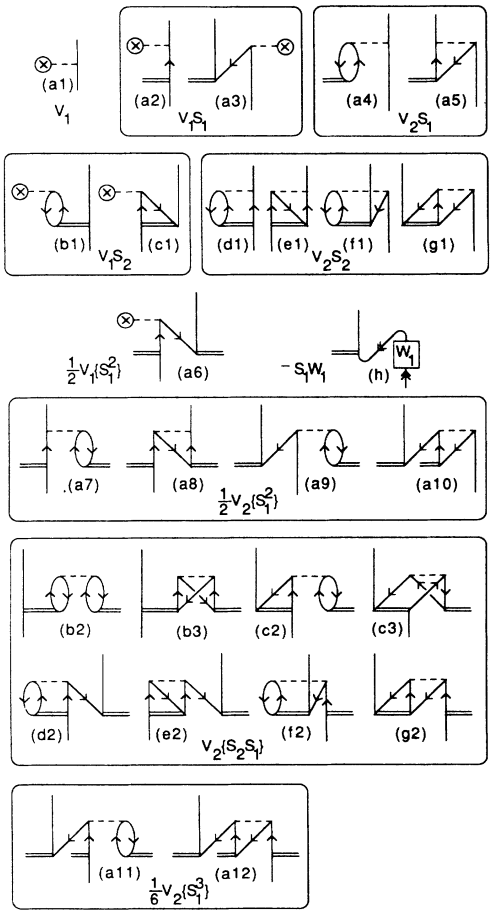

FIG. 2. All diagrams contributing to the right-hand side of the S_1 cluster equation. No arrows have been added on the incoming and outgoing lines. The incoming lines can be either core lines or valence lines. The diagrams are grouped according to from which term in Eq. (11) they originate. All diagrams building up a single diagram of Fig. 4, using the simplifying notation of Fig. 3, are labeled with the same letter but with different numbers.

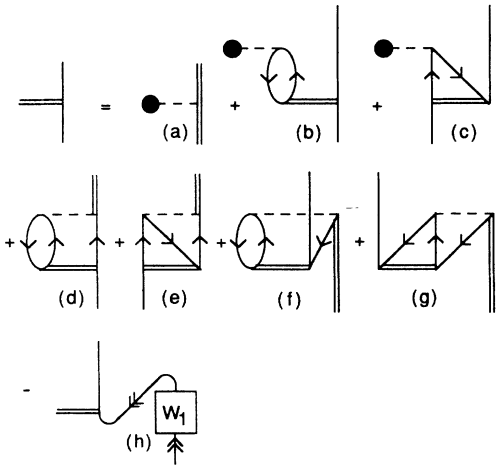

FIG. 4. Simplified diagrammatic form of the S_1 cluster equation using the notation of Fig. 3. All diagrams of Fig. 2 corresponding to a diagram in this figure are labeled with the same letter. No arrows have been added on the incoming and outgoing lines. The incoming lines can be either core lines or valence lines. The simplified diagrammatic notation of the cluster equation corresponds to similar simplifications in the evaluation of the diagrams.

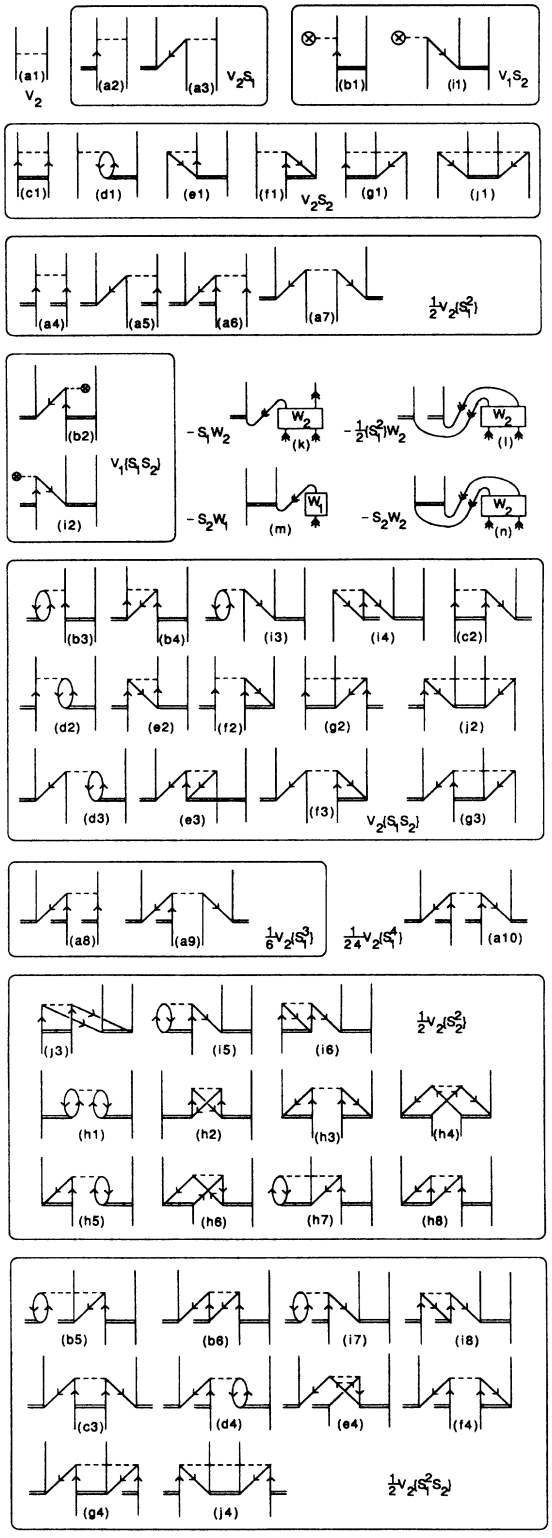

FIG. 5. All diagrams contributing to the right-hand side of the S_2 cluster equation. The diagrams are grouped according to from which term in Eq. (13) they originate. All diagrams building up a single diagram of Fig. 6 using the simplifying notation of Fig. 3 are labeled with the same letter but with different numbers.

$$[S_2,H_0]=Q\left\{V_2+V_2S_1+VS_2+\frac{1}{2!}V_2\{S_1^2\}+V\{S_1S_2\}\right.$$
$$+\frac{1}{3!}V_2\{S_1^3\}+\frac{1}{2!}V_2\{S_2^2\}+\frac{1}{2!}V_2\{S_1^2S_2\}$$
$$+\frac{1}{4!}V_2\{S_1^4\}-S_2W_1-S_1W_2$$
$$\left.-S_2W_2-\frac{1}{2!}\{S_1^2\}W_2\right\}_{2,c} \tag{13}$$

where the subscript 2 denotes that only double excitations are kept. All diagrams contributing to the RHS of Eq. (13) are given in Fig. 5. W_1 can, as mentioned, easily be evaluated as the P projection of the RHS of the S_1 equation. Also W_2 is easily achieved as the P projection of the RHS of the cluster equation for S_2 above

$$W_2=P\left\{V_2+V_2S_1+VS_2+\frac{1}{2!}V_2\{S_1^2\}+V\{S_1S_2\}\right.$$
$$+\frac{1}{3!}V_2\{S_1^3\}+\frac{1}{2!}V_2\{S_2^2\}+\frac{1}{2!}V_2\{S_1^2S_2\}$$
$$\left.+\frac{1}{2!}V_2\{S_1^4\}\right\}_{2,c}. \tag{14}$$

With the definitions of Fig. 3 the simplified S_2 equation of Fig. 6 is achieved with a large reduction of the number

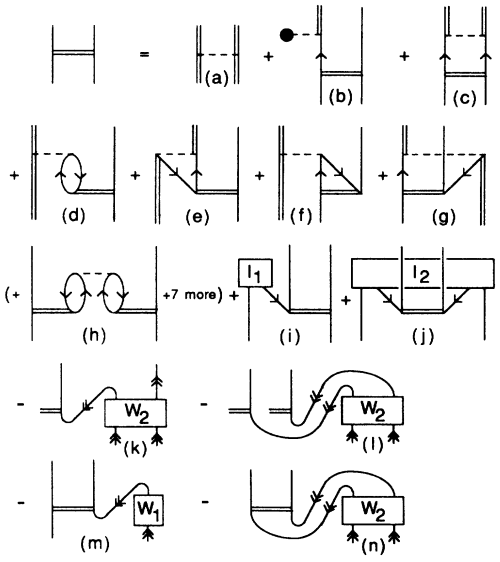

FIG. 6. Simplified diagrammatic form of the S_2 cluster equation using the notation of Fig. 3. All diagrams of Fig. 5 corresponding to a diagram in this figure are labeled with the same letter. No arrows have been added on the incoming and outgoing lines. The incoming lines can be either core lines or valence lines. The boxes denoted by I_1 and I_2 can be evaluated as overlaps of the S_1 and S_2 right-hand sides towards core orbitals. The simplified diagrammatic notation of the cluster equation corresponds to similar simplifications in the evaluation of the diagrams.

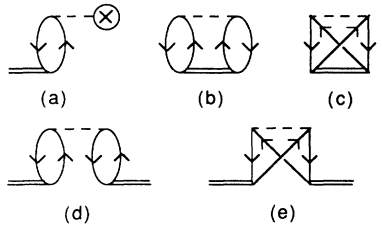

FIG. 7. Diagrams contributing to the total energy of a closed-shell system involving the S_1 and S_2 cluster operators. Using HF orbitals the first diagram, (a), does not contribute. Using HF orbitals the S_1 cluster occurs for the first time in second order of the perturbation expansion and thus the diagrams (d) and (e) occur for the first time in fifth order.

of diagrams to be considered. The labeling of the diagrams in Figs. 5 and 6 shows which diagrams from Fig. 5 are accounted for by the different diagrams in Fig. 6. The boxes in Fig. 6 denoted by I_1 and I_2 are easily evaluated as overlaps towards core orbitals of the RHS's of the S_1 and S_2 cluster equations, respectively.

Solving the coupled-cluster Eqs. (11) and (13) without any further approximations corresponds to the CCSD method. Earlier implementations of the CC method also neglected the effect of the S_1 cluster referred to as the CCD method. This corresponds to solving the S_2 cluster equation, Eq. (13), but only keeping the first term on the RHS's in the definitions of Fig. 3. The I_1 and W_1 boxes are still included though. The most complicated diagrams to evaluate originate from the $V_2\{S_2^2\}$ term in the RHS of S_2 equation giving rise to the diagrams (j3),(i5), (i6), and (h1)–(h8) shown in Fig. 5. The first tree, the factorizable ones, are easily included in the boxes I_1 and I_2 of Fig. 6 by evaluating overlaps towards core orbitals as described above. The remaining eight nonfactorizable ones, (h1)–(h8), are much more complicated to evaluate, however, and are often left out. This corresponds to the *factorizable* methods FCCSD including single excitations and FCCD if single excitations are left out. All four methods are explored in this work yielding the size of the effect of the single excitations and the nonfactorizable coupled-cluster diagrams.

The CCSD method has as mentioned been implemented for a general open-shell system as described above. The systems calculated in Sec. III are, however, closed-shell systems. For these systems the diagrams involving W_1 and W_2 are absent. For closed-shell systems the part of the total energy beyond *PHP*, i.e., $PVQ\Omega P$, corresponds to the zero-body part of W and is evaluated from the diagrams given in Fig. 7.

III. NUMERICAL RESULTS

In this section numerical results are presented for Be and Li^-, solving the coupled-cluster equations presented in Sec. II.

The single- and double-excitation clusters are in this work represented by single-particle and pair functions, respectively. To each occupied orbital being excited corresponds one single-particle function, having the same spin and angular symmetry. Each single-particle function is represented numerically by a radial function defined on a logarithmic radial lattice. The lattice is defined by $r=\exp(x)/Z$ with equidistantly distributed points in x between chosen minimum and maximum values $x_{\min}$ and $x_{\max}$ and Z is the nuclear charge. To represent a pair function, a partial-wave expansion is used. Each pair function, describing excitations from a specific pair of electrons, can then be represented by a series of radial pair functions, one for each angular symmetry. These radial pair functions are represented numerically on a two-dimensional radial lattice, using the same distribution of points in each radial coordinate as for the single-particle functions. Substituting the expansion of the pair functions into the coupled-cluster equations leads to a coupled system of equations for the radial single-particle and radial pair functions which in this work is solved by iterations to self-consistency.

The angular momentum algebra is performed using graphical techniques described in detail in the monograph by Lindgren and Morrison.[18] The resulting radial equations are solved by using finite discrete spectra as described in detail by Salomonson and Öster.[1]

All energies are in this work given in Hartree (hartree) atomic units where 1 hartree $=2$ Ry $\approx 27.211\,396$ eV.

A. Results for Be

In Table I second-order, third-order, and CCSD all-order results for the correlation energy of Be are presented. The second-order result represents 81.5% and the second- and third-order result 91.0% of the CCSD all-order result, showing the rather slow convergence using orbitals generated by the Hartree-Fock (HF) V^N potential.

Results are given explicitly for a number of partial-wave limits. From the higher calculated partial-wave limits the tail contribution from the remaining partial waves can be extrapolated. An asymptotic expression of the same form as in the helium case[1] is assumed for the partial-wave contributions

$$\Delta E_l = E_l - E_{l-1} = C_4(l+\tfrac{1}{2})^{-4} + C_5(l+\tfrac{1}{2})^{-5} + O(l^{-6}) \,. \tag{15}$$

This form is theoretically well established for helium.[21] The beryllium wave function fulfills the same cusp condition for antiparallel spin as the helium wave function and there is no reason to assume any differences in the asymptotic expression except for the size of the contributions.

The tail contribution is quite large for both the second-order and third-order correlation energies. The magnitude of the contribution from $l=11$ to ∞ is in both cases about 100 μhartree but with opposite sign. This gives rise to a peculiar behavior of the sum of the second- and third-order correlation energies having a maximum at $l=9$. The tail contribution for the CCSD correlation energy is 37 μhartree or 0.04% of the correlation energy, considerably smaller than in second order. The error in the tail contribution is believed to be less than 1 μhartree.

TABLE I. Second-order, third-order, and CCSD correlation energies for Be in different partial-wave l limits using HF orbitals. Correlation energies are given relative to $E_{HF}=-14.573\,023$ hartree. Energies given in μhartree.

l	Second order	Third order	Second plus Third order	CCSD
0	−15 930.9	−2 175.4	−18 106.3	−18 759.7
1	−64 349.6	−14 255.4	−78 605.0	−87 991.5
2	−72 139.0	−11 749.8	−83 888.8	−91 911.5
3	−74 430.9	−10 435.9	−84 866.8	−92 916.9
4	−75 328.2	−9 788.2	−85 116.4	−93 281.2
5	−75 746.8	−9 446.1	−85 192.9	−93 443.4
6	−75 966.9	−9 251.9	−85 218.8	−93 526.1
7	−76 093.2	−9 134.7	−85 227.9	−93 572.6
8	−76 170.7	−9 060.1	−85 230.8	−93 600.7
9	−76 220.8	−9 010.6	−85 231.4	−93 618.6
10	−76 254.5	−8 976.6	−85 231.1	−93 630.6
11	−76 278.1	−8 952.5	−85 230.6	
12	−76 295.1	−8 934.8	−85 229.9	
∞	−76 358	−8 867	−85 225	−93 667

In the helium case where the exact result is known, an error less than a few parts in 10^8 was achieved.[1] The numerical results were achieved using three different radial lattices with 81, 91, and 101 points, respectively, in the range $x_{min}=-7.6$ and $x_{max}=4.4$. Using a single lattice with say 101 points the numerical error is about 2 μhartree for the $l=10$ limit. To improve the numerical accuracy, lattice extrapolations can be performed using the formula[1]

$$E(h)=E(0)+ah^4+bh^5+O(h^6)\ , \tag{16}$$

where h is the lattice spacing. This is demonstrated in Table II. Using two lattices the numerical error is reduced to less than 0.1 μhartree. As a consistency check also lattice extrapolation results using three lattices are shown in Table II.

The contributions to the second-order and CCSD correlation energy from the different pair excitations and, for the CCSD case, the S_1^2 excitations are presented in Tables III and IV. The contributions from the $1s^2$ and $1s2s$ pairs are changed very little going from second order to CCSD. The $2s^2$ pair contribution, on the contrary increases by 50% and the $l>10$ tail contribution for this pair reduces drastically in magnitude from −58 to −4 μhartree.

The CCSD correlation energy also includes contributions from S_1^2 [see Figs. 7(d) and 7(e)] which are quite small. These represent, however, only a minor part of the effect of including the S_1 cluster and occur for the first time in fifth order of the perturbation expansion when HF orbitals are used. The main effect of the S_1 cluster comes from their modification of the S_2 cluster. For Be this effect is about 15 times larger than the direct contribution from the S_1^2 term and occurs for the first time in fourth order of the perturbation expansion.

To see explicitly the effect of the nonfactorizable S_2^2 diagrams and the effect of the S_1 cluster, results for the correlation energy in the different approximations discussed in Sec. II are presented in Table V. The effect of the nonfactorizable S_2^2 diagrams is very small and is evaluated in two ways as given in Table V. The result 28 μhartree is consistent with the result 3×10^{-5} hartree by Jeziorski *et al.*[22]

The effect of including S_1 has also been evaluated in two ways with the result −706 μhartree or 0.75% of the

TABLE II. Lattice extrapolation for the CCSD correlation energy in Be using HF orbitals. Energies given in μhartree.

l	81	91	101	81/91	91/101	81/91/101
0	−18 759.2	−18 759.4	−18 759.5	−18 759.8	−18 759.8	−18 759.7
1	−87 990.8	−87 991.1	−87 991.3	−87 991.7	−87 991.6	−87 991.5
2	−91 910.3	−91 910.8	−91 911.1	−91 911.7	−91 911.6	−91 911.5
3	−92 915.0	−92 915.8	−92 916.2	−92 917.1	−92 917.0	−92 916.9
4	−93 278.8	−93 279.8	−93 280.3	−93 281.4	−93 281.3	−93 281.2
5	−93 440.3	−93 441.6	−93 442.2	−93 443.6	−93 443.5	−93 443.4
6	−93 522.5	−93 523.9	−93 524.7	−93 526.3	−93 526.2	−93 526.1
7	−93 568.4	−93 570.0	−93 570.9	−93 572.7	−93 572.6	−93 572.6
8	−93 596.0	−93 597.7	−93 598.8	−93 600.7	−93 600.7	−93 600.7
9	−93 613.5	−93 615.4	−93 616.5	−93 618.5	−93 618.6	−93 618.6
10	−93 625.0	−93 627.1	−93 628.3	−93 630.5	−93 630.5	−93 630.6

TABLE III. Contributions from the different pair excitations to the second-order correlation energy in Be using HF orbitals. Energies given are in mhartree.

l	$1s^2$	$1s2s$	$2s^2$
0	−12 489	−1077	−2 366
1	−34 968	−4889	−24 492
2	−38 521	−5305	−28 313
3	−39 529	−5404	−29 498
4	−39 915	−5438	−29 976
5	−40 092	−5453	−30 203
6	−40 184	−5460	−30 323
7	−40 236	−5464	−30 393
8	−40 268	−5467	−30 436
9	−40 289	−5468	−30 464
10	−40 303	−5469	−30 483
∞	−40 345	−5472	−30 541

correlation energy. A decomposition into the different excitations of the effect of the nonfactorizable S_2^2 diagrams and the effect of the S_1 cluster is presented in Table VI. As expected the effect on excitations involving at least one $2s$ electron dominates heavily. For Be the contribution from S_1^2 is small compared to the total effect of single excitations as discussed above.

In Table VII a comparison with some other accurate calculations is presented. The numerical method used in the calculation of Lindgren and Salomonson[14] was based on direct numerical solution of partial differential equations.[23] This method is less accurate than the one used in this work.[1] The agreement with the present work in the CCD approximation is, however, very good. The second-order result, on the other hand, is off by 0.07 mhartree. An explanation of this might be the larger contributions from lattice and l-tail extrapolation in second order compared to all order, combined with the less accurate numerical method used in Ref. 14. Jankowski, Rutkowska, and Rutkowski[24] used for each partial wave a compact Slater-type orbitals (STO) basis set. As can be seen from a comparison between their results and our accurate ones their basis set error is about 0.08 mhartree and cancels to a large extent between the second- and third-order results. Jeziorski *et al.*[22] were using explicitly correlated Gaussian geminals to represent the pair functions. Their second- and third-order correlation energies are in excellent agreement with our results. Their CCD all-order correlation energy is, however, 0.10 mhartree above our result which is strange considering the agreement in second and third order. Alexander, Monkhorst, and Szalewicz[16] were also using correlated Gaussian-type geminals but with random tempering for optimization of their parameters. Their FCCD correlation energy is only 0.006 mhartree above our result which is an excellent agreement.

Our full CCSD result is also included in Table VII together with a recent Monte Carlo calculation of Umrigar, Wilson, and Wilkins[15] and the classical extensive CI calculation of Bunge.[13] Our CCSD result is comparable with the Monte Carlo calculation although the numerical uncertainty is larger in the Monte Carlo calculation.

In his original work,[13] Bunge reported a very good agreement between experiment and his theoretical result obtained by adding mass polarization effects, relativistic effects, and Lamb shift corrections to his nonrelativistic result for the total energy. In an erratum[13] Bunge later pointed out that the mass polarization energy had been added with the wrong sign. Correcting for this mistake gives a 60-μhartree difference between experiment and theory. A new revised comparison between theoretical and experimental results for Be is given by Mårtensson-Pendrill *et al.*[25] This investigation and results by Sundholm and Olsen[26] indicate that a large part of the 60-μhartree discrepancy is due to an underestimate by Bunge of the contribution from higher partial waves beyond the g limit.

The main part of the omitted effects in our calculation comes from the S_3 cluster. As is well known the ground state of Be has, in the multiconfiguration Hartree-Fock picture, a strong admixture of the nearly degenerate $1s^2 2p^2$ configuration which corresponds to a pair excitation in our language. The $1s2p$ correlation is thus an important S_3 effect. This effect has been calculated by Froese Fisher and Saxena[12] to −0.416 mhartree and should account for a large part of our omitted S_3 correlation. This is also the case as seen by comparing with the difference −0.638(25) mhartree between our CCSD result and the extensive CI result of Bunge. Our CCSD result, −93.667 mhartree, accounts for 99.3% of the total correlation energy, −94.305(25) mhartree, deduced from Bunge.

TABLE IV. Contributions from the different excitations to the CCSD correlation energy in different l limits for Be using HF orbitals. Energies given in μhartree.

	S_2			S_1^2
l	$1s^2$	$1s2s$	$2s^2$	
0	−13 936	−1243	−3 582	0.69
1	−38 134	−5189	−44 709	41.1
2	−41 191	−5591	−45 172	42.7
3	−41 988	−5675	−45 296	43.1
4	−42 280	−5702	−45 342	43.3
5	−42 411	−5714	−45 362	43.4
6	−42 478	−5719	−45 372	43.4
7	−42 516	−5722	−45 378	43.4
8	−42 539	−5724	−45 381	
9	−42 554	−5725	−45 384	
10	−42 563	−5726	−45 385	
∞	−42 593	−5728	−45 389	43.5

B. Comparison between HF and OHFS results for Be

When orbitals generated with a Hartree-Fock potential are used in the calculation of the correlation energy the effect of the single-excitation cluster S_1, appearing first in fourth order of the perturbation expansion, is small. Therefore the CCD approximation is rather good using such a potential. Using other potentials the effect of S_1

TABLE V. All-order correlation energies in various approximations for Be using HF orbitals. The effects of the nonfactorizable S_2^2 diagrams, and the single-excitation cluster S_1, are also given explicitly. Correlation energies are given relative to $E_{HF} = -14.573\,023$ hartree. Energies given in μhartree.

	FCCD[a]	CCD[b]	FCCSD[c]	CCSD[d]	Nonfactorizable S_2^2		Singles	
l	A	B	C	D	$B-A$	$D-C$	$D-B$	$C-A$
0	−18 713.7	−18 703.1	−18 770.6	−18 759.7	10.57	10.85	−56.6	−56.9
1	−87 355.3	−86 325.3	−88 022.2	−87 991.5	29.95	30.77	−666.1	−667.0
2	−91 246.6	−91 218.3	−91 940.5	−91 911.5	28.29	29.04	−693.1	−693.9
3	−92 244.5	−92 216.5	−92 945.5	−92 916.9	27.95	28.68	−700.3	−701.1
4	−92 606.1	−92 578.3	−93 309.8	−93 281.2	27.83	28.56	−702.9	−703.7
5	−92 767.1	−92 739.3	−93 471.9	−93 443.4	27.79	28.52	−704.1	−704.8
6	−92 849.2	−92 821.4	−93 554.6	−93 526.1	27.76	28.49	−704.7	−705.4
7	−92 895.3	−92 867.6	−93 601.1	−93 572.6	27.75	28.48	−705.0	−705.8
8	−92 923.2	−92 895.4	−93 629.2	−93 600.7			−705.2	−706.0
9	−92 941.0	−92 913.3	−93 647.1	−93 618.6			−705.4	−706.1
10	−92 952.9	−92 925.2	−93 659.1	−93 630.6			−705.4	−706.2
∞	−92 989	−92 961	−93 695	−93 667	27.7	28.5	−705.6	−706.4

[a]Factorizable coupled-cluster doubles (see Sec. II).
[b]Coupled-cluster doubles (see Sec. II).
[c]Factorizable coupled-cluster singles and doubles (see Sec. II).
[d]Coupled-cluster singles and doubles (see Sec. II).

TABLE VI. Change in the contributions to the correlation energy from different excitations due to the nonfactorizable S_2^2 diagrams (D-C from Tables V, IX) and due to the single excitations (C-A from Tables V,IX). Energies given in μhartrees.

		Be		Li^-	
		Nonfactorizable S_2^2	Singles	Nonfactorizable S_2^2	Singles
S_1^2	$2s\cdot 2s + 2s\cdot 1s$	−0.063	43.6	0.38	183.9
	$1s\cdot 2s + 1s\cdot 1s$	0.0001	−0.10	0.0003	−0.024
S_2	$1s^2$	0.96	44.8	1.18	47.3
	$1s2s$	−6.70	−151.2	−3.03	−178.8
	$2s^2$	34.3	−643.5	25.4	−925.5
Total		28.5	−706.4	23.9	−873.1

TABLE VII. Comparison with other calculations of the correlation energy for Be. Correlation energies are given relative to $E_{HF} = -14.573\,023$ hartree. Energies given in mhartree.

	This work	LS(80)[a]	JRR(82)[b]	JMSZ(84)[c]	AMS(88)[d]
Second order	−76.358	−76.28	−76.28	−76.35	
Third order	−8.867		−8.96	−8.86	
FCCD	−92.989	−93.00[e]		−92.89	−92.983
CCD	−92.961	−92.96[e]		−92.86	
FCCSD	−93.695				
CCSD	−93.667				
Monte Carlo	−93.4(3)[f]				
Full CI	−94.305(25)[g]				

[a]Lindgren and Salomonson (Ref. 14).
[b]Jankowski, Rutkowska, and Rutkowskii (Ref.24).
[c]Jeziorski *et al.* (Ref. 22).
[d]Alexander, Monkhorst, and Szalewicz (Ref. 16).
[e]In Ref. 14 the nonfactorizable S_2^2 diagrams were only calculated to lowest order giving the contribution +0.04 mhartree.
[f]From Umrigar, Wilson, and Wilkins (Ref. 15).
[g]From Bunge (Ref. 13). The final result was obtained by adding the estimated STO basis function error −0.407(23) mhartree and the full CI truncation error −0.019(2) mhartree to the full CI correlation energy of 93.879 mhartree.

TABLE VIII. Comparison between using orbitals generated with a HF or an OHFS potential when calculating the total energy for Be in the CCSD approximation. The contributions from different excitations are given explicitly. Energies given in mhartree.

		HF	OHFS
E_{HF}/E_{OHFS}		−14 573.02	−14 544.71
S_1	$1s$	0	−1.49
	$2s$	0	−23.15
S_1^2		0.04	0.86
S_2	$1s^2$	−42.59	−42.04
	$1s2s$	−5.73	−7.13
	$2s^2$	−45.39	−48.94
Total		−14 666.69	−14 666.60

on the correlation energy occurs already in second order. This makes it essential to use the CCSD method using such potentials. To demonstrate this we have made a calculation with an "optimized" Hartree-Fock-Slater (OHFS) potential[27,28] of the $1s^22s$ Be^+ configuration. In this potential a local approximation of the exchange interaction is made:

$$V_{OHFS}(r)=\frac{Z(r)}{r}-\frac{3C}{2r}\left[\frac{3r^n\rho(r)}{4\pi^2}\right]^{1/3} \tag{17}$$

where we have chosen $C=0.8$ and $n=1.15$ and $\rho(r)$ is the radial electron charge density and $Z(r)/r$ accounts for the direct interaction.

A comparison between the HF and OHFS calculations is given in Table VIII where the contributions to the total energy from the different excitations are presented. On the first line the expectation value of the total Hamiltonian using Ψ_0 is given showing quite a large difference between the two calculations to be recovered by the CCSD expansion. As seen in the table the main part of the difference comes from the S_1 excitation [Fig. 7(a)] involving the $2s$ electron giving −23.15 mhartree. All the S_1, S_1^2, and S_2 excitations are, however, important to resolve the difference in the expectation value of Ψ_0 leaving a difference of only 0.09 mhartree or 0.1% of the correlation energy. This remaining difference is of course mainly due to the difference in the contribution from the S_3 cluster.

C. Results for Li^-

The negative lithium ion has the same configuration as beryllium but the $2s$ electrons are much more loosely bound and the size of Li^- is therefore much larger. A preliminary comparison between the two systems concerning total energies, detachment energies, and geometrical properties has recently been made[29] showing large similarities between the two systems despite their different sizes. To cover the range of the Li^- system, larger lattices than for Be were used with $x_{min}=-7.6$ and $x_{max}=5.4$. As for Be three different lattices with 81, 91, and 101 points were used in this range for lattice extrapolation and consistency check of this extrapolation. The direct iteration of the coupled-cluster equations, including singles and doubles, was found to diverge. To achieve convergence it was necessary to apply a damping factor between the iterations.

The correlation energies in the different approximations discussed in Sec. II are for Li^- presented in Table IX. The effect of the nonfactorizable coupled-cluster diagrams and the effect of single excitations are also extracted in this table and are found to have the same size as for Be. The more detailed decomposition of these effects presented in Table VI reveals, however, that the effect of S_1 is much more important for Li^- than for Be. The contribution from S_1^2 is more than four times larger for Li^- but is compensated by an even larger change of the S_2 contribution due to inclusion of the S_1 cluster. A peculiarity of Li^- is that the s-limit results are very sensitive to the inclusion of singles as seen in Table IX.

The contributions to the correlation energy from the

TABLE IX. All-order correlation energies in various approximations for Li^- using HF orbitals. The effects of the nonfactorizable S_2^2 diagrams, and the single-excitation cluster S_1, are also given explicitly. Correlation energies are given relative to $E_{HF}=-7.428\,232$ hartree. Energies given in μhartree.

	FCCD	CCD	FCCSD	CCSD	Nonfactorizable S_2^2		Singles	
l	A	B	C	D	$B-A$	$D-C$	$D-B$	$C-A$
0	−22 747.6	−22 700.9	−24 010.5	−23 941.0	46.74	69.48	−1240.1	−1262.9
1	−66 972.2	−66 944.6	−67 798.7	−67 774.0	27.63	24.74	−829.4	−826.5
2	−69 964.7	−69 937.6	−70 823.9	−70 799.8	27.14	24.13	−862.2	−859.2
3	−70 727.0	−70 700.0	−71 594.4	−71 570.5	27.03	23.99	−870.5	−867.4
4	−71 002.5	−70 975.5	−71 872.8	−71 848.8	27.00	23.95	−873.4	−870.3
5	−71 124.9	−71 097.9	−71 996.4	−71 972.5	26.97	23.93	−874.6	−871.6
6	−71 187.2	−71 160.3	−72 059.4	−72 035.5	26.96	23.92	−875.2	−872.2
7	−71 222.3	−71 195.3	−72 094.8	−72 070.9			−875.6	−872.5
8	−71 243.5	−71 216.5	−72 116.2	−72 092.3			−875.8	−872.7
9	−71 257.0	−71 230.0	−72 129.8	−72 105.9			−875.9	−872.9
∞	−71 293	−71 266	−72 166	−72 142	26.9	23.9	−876.2	−873.1

TABLE X. Contributions from the different excitations to the CCSD correlation energy in different l limits for Li^- using HF orbitals. Energies given in μhartree.

l	$1s^2$	S_2 $1s2s$	$2s^2$	S_1^2
0	−15 430	−494	−8 180	163.0
1	−38 769	−2305	−26 873	173.4
2	−41 548	−2463	−26 970	181.0
3	−42 259	−2494	−27 000	182.9
4	−42 517	−2504	−27 012	183.6
5	−42 632	−2508	−27 017	183.9
6	−42 691	−2510	−27 019	184.0
7	−42 724	−2511	−27 020	184.1
8	−42 744	−2511	−27 021	184.1
9	−42 756	−2512	−27 022	184.2
∞	−42 790	−2513	−27 023	184.3

different excitations are given in Table X. These can be compared with the corresponding ones for Be in Table IV. The $1s^2$ correlation energy is almost identical for Be and Li^-. The $1s2s$ and $2s^2$ correlation energies on the other hand, are much smaller for Li^- than for Be. The conclusion that the $2s^2$ correlation is less important in Li^- is not correct, however. Comparing with the $F^0(2s^2)$ integral having the value 162.8 mhartree for Li^- and 343.2 mhartree for Be one can see that the relative importance of correlation in the $2s$ shell is larger for Li^- than for Be.

In Table XI an attempt to estimate the total "experimental" nonrelativistic energy of Li^- is made. This estimate is based on the accurate nonrelativistic calculation for Li^+ by Pekeris[30] and the experimental values of the ionization potential[31] (IP) and electron affinity[32,33] (EA) of Li corrected for mass polarization and relativistic effects. The mass polarization effect in the IP was taken from the measurement by Lorenzen and Niemax[34] while the corresponding effect in the EA was assumed to be negligible compared to the accuracy achieved. Relativistic effects were estimated from Hartree-Fock and Dirac-Fock calculations. An error of 50% of the relativistic effects was assigned to account for the neglected effects of the Breit interaction, relativistic correlation, and Lamb shift. This size of the error is based on calculations on Be showing a reduction of the relativistic corrections by about 40% including these effects.[25] The final result for the total energy of Li^-, −7500.78(3) mhartree, is somewhat larger in magnitude than the value −7500.40(20) estimated from CI calculations by Sims *et al.*[35]

A comparison with other accurate calculations and with ours, from experimental results, estimated nonrelativistic energy is made in Table XII. Our CCSD calculation accounts for 99.4(1)% of the nonrelativistic correlation energy, a result strikingly similar to the Be result giving 99.3% of the correlation energy. Comparing with the CCSD calculation of Canuto *et al.*[36] using a Gaussian-type basis set one clearly sees a basis set error of about 6 mhartree in their calculation. A large part of this error, however, is probably due to a poor description of the $1s^2$ shell and does not influence the $2s^2$ shell so much. Canuto *et al.* have also calculated the effect of the S_3 cluster in an approximate way giving −0.2 mhartree, but the numerical error in this value might be large since the $1s$ core is not so well described. This value can be compared with the difference −0.4 mhartree between the estimated nonrelativistic energy and our CCSD calculation. Comparing with the combined CI-Hylleraas calculation of Sims *et al.*[35] and the Monte Carlo calculation of Umrigar *et al.*[37] our CCSD calculation account for a slightly larger part of the correlation energy.

The experimental electron affinity of Li is 22.7 mhartree while the correlation energy of Li^- is a factor of 3

TABLE XI. Estimation of the total nonrelativistic energy of Li^- using the experimental ionization potential E_{IP} and the electron affinity E_{EA} of Li. Energies given in mhartree.

$E(Li^+)$[a]	−7279.913
$-E_{IP}=[E(Li)-E(Li^+)]$[b]	−198.157
Mass polarization[c]	−0.001
Relativistic effects[d]	+0.016
$-E_{EA}=[E(Li^-)-E(Li)]$[e]	−22.71(2)
Relativistic effects[d]	−0.001
$E(Li^-)$[f]	−7500.78(3)

[a]The nonrelativistic energy of Li^+ $1s^2$ calculated by Pekeris (Ref. 30).

[b]Experimental ionization potential 198.142 mhartree of Li from Moore's Tables (Ref. 31) corrected for the normal mass shift of ^{7}Li.

[c]Experimental mass polarization from Lorenzen and Niemax (Ref. 34).

[d]Relativistic corrections evaluated as the difference between Dirac-Fock and Hartree-Fock calculations.

[e]Experimental electron affinity recommended by Hotop and Lineberger (Ref. 33) mainly based on the experiment by Feldmann (Ref. 32).

[f]Total estimated nonrelativistic energy of Li^-. The uncertainty includes a rough estimate of the error in the relativistic effects between Li^- and Li^+ due to the neglect of the Breit interaction, relativistic correlation, and Lamb shift (see text).

TABLE XII. Comparison with other calculations of the total nonrelativistic energy for Li^-. Correlation energies are given relative to $E_{HF}=-7.428\,232$ hartree. Energies given in mhartree.

	Correlation	Total energy
This work CCSD[a]	−72.142	−7500.374
CCSD[b]	−65.9	−7494.1
CI-Hylleraas[c]	−71.96	−7500.19
Monte Carlo[d]	−71.6(1)	−7499.8(1)
Expt.[e]	−72.55(3)	−7500.78(3)

[a]Using numerical finite discrete spectra.

[b]Using a Gaussian-type basis set (Ref. 36).

[c]Combined CI-Hylleraas calculations from Sims *et al.* (Ref. 35).

[d]From Umrigar, Wilson, and Wilkins (Ref. 37).

[e]Estimated nonrelativistic energy deduced in Table XI.

larger. Since the total energy of Li is calculated with high accuracy,[38,39] the main error in an evaluation of the electron affinity would come from the omitted effects of the S_3 cluster on the correlation energy for Li^-. As shown above these effects amount to about 0.6% of the Li^- correlation energy and thus to about 1.8% for the Li electron affinity. The CCSD method thus accounts for 98.2% of the electron affinity of Li.

IV. SUMMARY AND CONCLUSION

In this work we have presented an implementation of the coupled-cluster single- and double-excitation method. The presentation is based on a diagrammatic notation. Redefinition of incoming and outgoing electron lines and of the effective potential interaction leads to a great simplification of the diagrammatic expression of the cluster equations for single and double excitations and also to a more efficient evaluation scheme.

We have in this work solved the coupled-cluster equations in the CCSD approximation by using numerical discrete spectra.[1] Our results show that a truncation error less than 1 μhartree is easily obtained using this method. We here emphasize the importance of using computational methods giving truncation errors smaller than the omitted physical effects.

Calculations have been performed for the total energy of Be and Li^-. The CCSD method was found to account for 99.3% and 99.4% of the correlation energy for these systems, respectively. The main part of the omitted effects comes from the triple-excitation cluster. Also performed is a comparison between calculations using Hartree-Fock spectra and Hartree-Fock-Slater spectra. This comparison shows that the total energy depends very little on the potential used in defining the perturbation expansion when the CCSD method is used. The reason for this is the inclusion of all powers of the S_1 cluster accounting for single excitations. This is advantageous since using other potentials than the HF potential might be more physical and might improve convergence properties. So far we have presented calculations on heliumlike[1] and berylliumlike systems. However, our intention is to use the CCSD method for heavier atoms where relativistic effects are important. We have therefore also developed a relativistic CCSD program[2] and calculations on heavier atoms are planned to be presented in forthcoming papers.

ACKNOWLEDGMENTS

The authors wish to acknowledge their colleagues Ingvar Lindgren, Jean-Louis Heully, Ann-Marie Mårtensson-Pendrill, and Eva Lindroth for stimulating discussions and comments on the manuscript. This work has been supported by the Swedish Natural Science Research Council.

[1]Sten Salomonson and Per Öster, Phys. Rev. A **40**, 5559 (1989).
[2]Sten Salomonson and Per Öster, Phys. Rev. A **40**, 5548 (1989).
[3]Jiří Čížek, J. Chem. Phys. **45**, 4256 (1966); Adv. Chem. Phys. **14**, 35 (1969).
[4]George D. Purvis III and Rodney J. Bartlett, J. Chem. Phys. **76**, 1910 (1982).
[5]Azizul Haque and Uzi Kaldor, Int. J. Quantum Chem. **29**, 425 (1986).
[6]Gustavo E. Scuseria, Andrew C. Scheiner, Timothy J. Lee, Julia E. Rice, and Henry F. Schaefer, III, J. Chem. Phys. **86**, 2881 (1987).
[7]Miroslav Urban, Vladimir Kellö, Ivan Cernusak, Jozef Noga, and Geerd H. F. Diercksen, Chem. Phys. Lett. **135**, 346 (1987).
[8]Jozef Noga and Rodney J. Bartlett, J. Chem. Phys. **86**, 7041 (1987); **89**, 3401(E) (1988).
[9]Gustavo E. Scuseria and Henry F. Schaefer III, Chem. Phys. Lett. **152**, 382 (1988).
[10]H. M. Quiney, I. P. Grant, and S. Wilson, in *Many-Body Methods in Quantum Chemistry,* Vol. 52 of *Lecture Notes in Chemistry,* edited by U. Kaldor (Springer, Berlin, 1989), p. 331.
[11]Hugh P. Kelly, Phys. Rev. **131**, 684 (1963).
[12]C. Froese Fischer and K. M. S. Saxena, Phys. Rev. A **9**, 1498 (1974).
[13]Carlos F. Bunge, Phys. Rev. A **14**, 1965 (1976); **17**, 486(E) (1978).
[14]Ingvar Lindgren and Sten Salomonson, Phys. Scr. **21**, 335 (1980).
[15]C. J. Umrigar, K. G. Wilson, and J. W. Wilkins, Phys. Rev. Lett. **60**, 1719 (1988).
[16]S. A. Alexander, H. J. Monkhorst, and K. Szalewicz, J. Chem. Phys. **89**, 355 (1988).
[17]H. Kümmel, K. H. Lührmann, and J. G. Zabolitzky, Phys. Rep. **36**, 1 (1978).
[18]I. Lindgren and J. Morrison, *Atomic Many-Body Theory,* 2nd ed. (Springer-Verlag, Berlin, 1986).
[19]Ann-Marie Mårtensson-Pendrill and Anders Ynnerman, Phys. Scr. **41**, 329 (1990).
[20]Ingvar Lindgren, Int. J. Quantum Chem. **S12**, 33 (1978).
[21]Rober Nyden Hill, J. Chem. Phys. **83**, 1173 (1985).
[22]Bogumil Jeziorski, Hendrik J. Monkhorst, Krzysztof Szalewicz, and John G. Zabolitzky, J. Chem. Phys. **81**, 368 (1984).
[23]Ann-Marie Mårtensson, J. Phys. B **12**, 3995 (1979).
[24]K. Jankowski, D. Rutkowska, and A. Rutkowski, J. Phys. B **15**, 4063 (1982).
[25]Ann-Marie Mårtensson-Pendrill, Steve Alexander, Ludwik Adamowicz, Nevin Oliphant, Jeppe Olsen, Per Öster, Harry M. Quiney, Sten Salomonson, and Dage Sundholm (unpublished).
[26]D. Sundholm and J. Olsen (unpublished).
[27]Ingvar Lindgren, Ark. Fys. **31**, 59 (1966).
[28]Arne Rosén and Ingvar Lindgren, Phys. Rev. **176**, 114 (1968).
[29]Jean-Louis Heully and Sten Salomonson, Phys. Scr. **38**, 143 (1988).
[30]C. L. Pekeris, Phys. Rev. **112**, 1649 (1958).
[31]Charlotte E. Moore, *Atomic Energy Levels* (National Bureau of Standards, Washington, D.C., 1949) (reissued 1971), Vol. I, Circ. 467.
[32]D. Feldmann, Z. Phys. A **277**, 19 (1976).
[33]H. Hotop and W. C. Lineberger, J. Phys. Chem. Ref. Data **14**,

731 (1985).
[34]C.-J. Lorenzen and K. Niemax, J. Phys. B **15**, L139 (1982).
[35]James S. Sims, Stanley A. Hagstrom, David Munch, and Carlos F. Bunge, Phys. Rev. A **13**, 560 (1976).
[36]S. Canuto, W. Duch, J. Geertsen, F. Müller-Plathe, J. Oddershede, and G. E. Scuseria, Chem. Phys. Lett. **147**, 435 (1988).
[37]C. J. Umrigar, K. G. Wilson, and J. W. Wilkins, in *Computer Simulation Studies in Condensed Matter Physics: Recent Developments,* edited by D. P. Landau and H. B. Schuttler (Springer-Verlag, Berlin, 1988).
[38]Ingvar Lindgren, Phys. Rev. A **31**, 1273 (1985).
[39]S. A. Blundell, W. R. Johnson, Z. W. Liu, and J. Sapirstein, Phys. Rev. A **40**, 2233 (1989).